Atmos. Meas. Tech. Discuss., 6, 7771–7810, 2013
www.atmos-meas-tech-discuss.net/6/7771/2013/
doi:10.5194/amtd-6-7771-2013
© Author(s) 2013. CC Attribution 3.0 License.

Atmospheric Measurement Techniques
Open Access
Discussions

This discussion paper is/has been under review for the journal Atmospheric Measurement Techniques (AMT). Please refer to the corresponding final paper in AMT if available.

Propagation of radiosonde pressure sensor errors to ozonesonde measurements

R. M. Stauffer[1], G. A. Morris[2], A. M. Thompson[1,3], E. Joseph[4], and G. J. R. Coetzee[5]

[1]Department of Meteorology, The Pennsylvania State University, University Park, Pennsylvania, USA
[2]Department of Physics and Astronomy, Valparaiso University, Valparaiso, Indiana, USA
[3]NASA/Goddard Space Flight Center, Greenbelt, Maryland, USA
[4]Department of Physics and Astronomy, Howard University, Washington, D.C., USA
[5]South African Weather Service, Pretoria, South Africa

Received: 26 July 2013 – Accepted: 11 August 2013 – Published: 26 August 2013

Correspondence to: R. M. Stauffer (rms5539@psu.edu)

Published by Copernicus Publications on behalf of the European Geosciences Union.

Abstract

Several previous studies highlight pressure (or equivalently, pressure altitude) discrepancies between the radiosonde pressure sensor and that derived from a GPS flown with the radiosonde. The offsets vary during the ascent both in absolute and percent pressure differences. To investigate this, a total of 501 radiosonde/ozonesonde launches from the Southern Hemisphere subtropics to northern mid-latitudes are considered, with launches between 2006–2013 from both historical and campaign-based intensive stations. Three types of electrochemical concentration cell (ECC) ozonesonde manufacturers (Science Pump Corporation; SPC and ENSCI/Droplet Measurement Technologies; DMT) and five series of radiosondes from two manufacturers (International Met Systems: iMet, iMet-P, iMet-S, and Vaisala: RS80 and RS92) are analyzed to determine the magnitude of the pressure offset and the effects these offsets have on the calculation of ECC ozone (O_3) mixing ratio profiles (O_{3MR}) from the ozonesonde-measured partial pressure. Approximately half of all offsets are $> \pm 0.7$ hPa in the free troposphere, with nearly a quarter $> \pm 1.0$ hPa at 26 km, where the 1.0 hPa error represents ~5 % of the total atmospheric pressure. Pressure offsets have negligible effects on O_{3MR} below 20 km (98 % of launches lie within ±5 % O_{3MR} error at 20 km). Ozone mixing ratio errors in the 7–15 hPa layer (29–32 km), a region critical for detection of long-term O_3 trends, can approach greater than ±10 % (> 25 % of launches that reach 30 km exceed this threshold). Comparisons of total column O_3 yield average differences of +1.6 DU (−1.1 to +4.9 DU 10th to 90th percentiles) when the O_3 is integrated to burst with addition of the McPeters and Labow (2012) above-burst O_3 column climatology. Total column differences are reduced to an average of +0.1 DU (−1.1 to +2.2 DU) when the O_3 profile is integrated to 10 hPa with subsequent addition of the O_3 climatology above 10 hPa. The RS92 radiosondes are clearly distinguishable in performance from other radiosondes, with average 26 km errors of +0.32 hPa (−0.09 to +0.54 hPa 10th to 90th percentiles) or −1.31 % (−2.19 to +0.37 %) O_{3MR} error. Conversely, iMet-P radiosondes had average 26 km errors of −1.49 hPa

AMTD
6, 7771–7810, 2013

Propagation of radiosonde pressure sensor errors

R. M. Stauffer et al.

CC BY

(−2.33 to −0.82 hPa) or +6.71 % (+3.61 to +11.0 %) O_{3MR} error. Based on our analysis, we suggest that ozonesondes always be coupled with a GPS-enabled radiosonde and that pressure-dependent variables, such as O_{3MR}, be recalculated/reprocessed using the GPS-measured altitude, particularly when 26 km pressure offsets exceed ±1.0 hPa/±5 %.

1 Introduction

A number of fundamental intercomparison studies about radiosonde (e.g., Nash et al., 2006; da Silveira et al., 2006) and ozonesonde (e.g., Smit et al., 2007; Deshler et al., 2008) instrument performance have appeared within the past two decades. Radiosonde investigations have focused on comparisons of instrument type with respect to temperature (Gaffen, 1994; Gaffen et al., 1999; Miloshevich et al., 2006; Steinbrecht et al., 2008; Sun et al., 2010), humidity (Vömel et al., 2007; Yoneyama et al., 2008; Miloshevich et al., 2006; Sun et al., 2010) and pressure (Inai et al., 2009; Hurst et al., 2011) measurements and typically have been associated with the adoption of new sonde models. The performance of electrochemical concentration cell (ECC) ozonesonde instruments, of which there have been three manufacturers since the 1970s, has been compared with various compositions of sensing solution type in laboratory conditions (Smit and Kley, 1998; Smit et al., 2007, 2011), and field conditions (Komhyr et al., 1995a,b; Thompson et al., 2007; Deshler et al., 2008). The discrepancies among the ozonesonde instrument-sensing-solution combinations are ∼ 5–15 % relative to an absolute O_3 measurement, depending on ECC manufacturer, and are pressure (and thus, altitude)-dependent. The O_3 community has made many attempts to homogenize standard operational procedures (Deshler, 2012; WMO, 2013) for station pre-flight preparations and intercomparison of different ECC cells, so some of these variables are well understood. At present, the global ozonesonde community is reprocessing thousands of O_3 profiles from dozens of stations to produce a more accurate profile dataset for

AMTD
6, 7771–7810, 2013

cc BY

trends analysis. Importantly, in this effort, the pressure measured by the radiosonde to which the O_3 partial pressure is referenced, has been taken as a fixed parameter.

The relatively recent widespread use of GPS-enabled radiosondes has shown that pressure sensors often differ from the pressure derived from the GPS data. These errors can propagate to errors in the calculated O_3 mixing ratio (O_{3MR}, or equivalently, concentration).

1.1 Efforts to quantify radiosonde errors and biases

Numerous intercomparison studies exist that investigate biases in the pressure, temperature, humidity and GPS measurements amongst various radiosonde types. da Silveria et al. (2006) launched five types of GPS-enabled radiosondes in groups to analyze GPS measurements in addition to meteorological measurements. They found the reproducibility and comparisons of GPS altitude in the stratosphere were within ±20 m. Hurst et al. (2011) compared RS92 and iMet pressure measurements and found that paired RS92 radiosondes all compared to within ±0.3 hPa in the stratosphere and that iMet radiosondes averaged approximately 0.8 hPa lower than the RS92s between 25–30 km, an error of > 5 %. Inai et al. (2009) studied individual RS80 radiosonde launches to compare pressure derived from GPS measurements with the radiosonde pressure sensor and found pressure sensor biases of −0.5 hPa above 20 km. These pressure errors need to be considered in the context of O_{3MR} measurements and total column O_3 integration.

Lately, radiosonde manufacturers (e.g., Lockheed Martin Sippican, Inc., GPS Mark II Microsonde) have been producing radiosondes without pressure sensors, relying on GPS altitude, temperature, and humidity measurements and the hydrostatic equation to derive pressure data. This same technique is used in this study and will be described below.

AMTD
6, 7771–7810, 2013

1.2 Importance of accurate O_3 measurements

The importance of long-term, accurate O_3 profile records is well-documented in climate reports (IPCC, 2007), O_3 assessment reports (WMO, 2011), and numerous studies of trends in tropospheric (Logan et al., 1994, 1999; IPCC, 2007), stratospheric (Miller et al., 1995; Froidevaux et al., 1996; Liu et al., 2006; Rault et al., 2007; Jiang et al., 2007; Kroon et al., 2011) and total column O_3 (Thompson et al., 2003; Osterman et al., 2008). Furthermore, ozonesondes provide the highest vertical resolution ($\sim$ 10 m or less) O_3 measurements from the surface to over 30 km. For this reason, the satellite remote sensing community preferably uses ozonesonde profile data for validation and improvement of O_3 profile retrievals (e.g., Nalli et al., 2013). Additionally, the absolute accuracy of radiosonde measured pressure profiles themselves also has potential ramifications in the validation of satellite-derived pressure-profile environmental data records (EDRs; Nalli et al., 2013).

Biases in O_3 measurements from the use of several different types of ECC ozonesonde manufacturers, as well as different potassium iodide sensing solution strengths and sonde preparation techniques have made the homogenization of the historical ozonesonde record a necessity. The goals of the homogenization process are to compile the highest accuracy O_3 profile records for more robust trends studies and satellite comparisons (Deshler, 2012). With the ongoing reprocessing of ozonesonde data, it is vital to identify every potential bias or error in the O_3 measurements.

In the present investigation a series of 394 ozonesonde-radiosonde instrument packages and 107 RS92 radiosondes flown solo have been analyzed. In this paper, we address the following questions:

1. What are the statistical characteristics for pressure differences ("offsets") between the pressure sensor and that derived from the GPS? How do the offsets vary as a function of pressure (altitude)?

AMTD
6, 7771–7810, 2013

cc BY

2. How do the offsets vary between radiosonde models? In this study, we analyze the RS80 flown with an attached GPS, the RS92, and three versions of International Met Systems (iMet) radiosondes.

3. In addition to pressure offsets, some of the radiosondes demonstrate highly variable pressure measurements during ascent, especially in the stratosphere. What are the statistical characteristics of this variability?

4. How do the radiosonde pressure offsets propagate to the O_3 profiles? How is integrated total O_3 to either the balloon burst altitude or a pressure cut-off (e.g., ∼ 11 hPa/∼ 30 km, as recommended in Dobson, 1973 or 10 hPa, as utilized in Thompson et al., 2003, 2007), and an extrapolated add-on determined from a climatology like McPeters and Labow (2012) affected?

The soundings were taken in the 2006–2013 period in a range of locations from the northern mid-latitudes through the subtropics and tropics to southern subtropics (Table 1).

2 Methodology

2.1 Site and instrument descriptions

A total of 501 radiosondes were analyzed for this study, with ozonesonde/radiosonde pairs accounting for 394 of those profiles. Our analysis includes data from eleven different launch sites (including two simultaneously operated, closely located sites in Houston, TX) launching five types of radiosondes, and spanning the years 2006–2013 (Table 1). The locations range from the southern subtropics (Irene; –25.91°/28.21°) to the northern mid-latitudes (Sapporo; 43.07°/141.35°) with every month of the year represented. Stations include both those making regular ozonesonde launches (Irene, Houston, Beltsville) and those involved in intensive launching for specific campaigns (Las Tablas, Panama, TC[4]: Tropical Composition, Cloud, and Climate Coupling, http://www.nasa.gov/mission_pages/TC4/; Houston, TX and the Research Vessel *Ronald H. Brown* (herein RHB), IONS-06: INTEX-B Ozonesonde Network Study 2006, http://croc.gsfc.nasa.gov/intexb/ions06.html; Edgewood, MD and Porterville, CA, DISCOVER-AQ: Deriving Information on Surface Conditions from Column and Vertically Resolved Observations Relevant to Air Quality, http://www.nasa.gov/mission_pages/discover-aq/index.html), as well as other profiling missions at other sites.

Two radiosonde types from Vaisala (Vantaa, Finland; RS80, RS92) and three from International Met Systems (Grand Rapids, MI, USA; iMet, iMet-P, iMet-S) were launched at the various locations. Analyses are presented for each radiosonde type. The number of launches of each radiosonde type and the manufacturer-quoted pressure accuracies/uncertainties are given in Table 2. International Met Systems uses a piezoresistive silicon device to measure pressure and quotes only one pressure accuracy throughout the manufacturing of their radiosondes from 2009–2013. The analyses are still presented by each series type (based on serial numbers that are, in general, temporally partitioned) to determine any differences throughout the evolution of iMet radiosonde production. The RS92 radiosondes received a significant pressure sensor upgrade from the RS80s, moving from an aneroid capacitor, which is observed to have a low bias in the stratosphere (Steinbrecht et al., 2008), to a more accurate solid-state silicon barocap sensor.

2.2 Ozonesonde measurements

Each of the Science Pump Corporation (SPC) and ENSCI/Droplet Measurement Technologies (DMT) ozonesondes in this study operate using the electrochemical concentration cell (ECC; Komhyr, 1969) technique where ambient air is bubbled through a potassium iodide solution. The subsequent reactions generate two electrons per O_3 molecule, so the current measured through an attached circuit board is proportional to the O_3 partial pressure (pO_3). Since O_{3MR} is calculated from the pO_3 and total air pressure, p

AMTD
6, 7771–7810, 2013

Propagation of radiosonde pressure sensor errors

R. M. Stauffer et al.

$$O_{3MR} = pO_3/p_{air} \tag{1}$$

any bias or error in the radiosonde pressure measurement introduces error in O_{3MR}. The pO_3 measurements have typical tropospheric accuracies on the order of −7 to +17 %, improving to ±5 % in the low to mid-stratosphere with decreasing accuracy above 10 hPa, provided standardized and accepted ozonesonde conditioning and launch procedures are followed (Komhyr et al., 1995b; WMO, 2013).

2.3 Calculation of GPS pressure

The pressure altitude reported by the radiosonde is given in geopotential height (Z), using standard gravity ($g_0 = 9.80665\,\mathrm{ms^{-2}}$). Conversely, the GPS altitude is reported as a geometric height (H), and the latitude-dependent gravity ($g \approx 9.78$–$9.83\,\mathrm{ms^{-2}}$) is used to calculate pressure. This is the reverse process of obtaining a geopotential height from the radiosonde pressure measurements, but with a geometric altitude. We note that the reported GPS altitude is actually an ellipsoidal height, though the difference between that and height AMSL (geoidal height; National Imagery and Mapping Agency, 2000, see p. 68) is reconciled with the input of the station AMSL height as the initial GPS altitude prior to launch. Surface pressure from the radiosonde (often set at the launch site from a high-precision barometer) is used to initialize the GPS pressure calculation from a form of the hydrostatic equation:

$$p_{\mathrm{GPS}i} = p_{\mathrm{GPS}i-1}\exp\left[-\frac{g\Delta H}{R_\mathrm{d}T_\mathrm{vavg}}\right]. \tag{2}$$

Here, p_{GPS} is the pressure calculated from g, the latitude-dependent gravity, ΔH, the change in geometric GPS height from consecutive measurements, $\mathrm{R_d}$, the specific gas constant for dry air (287.05 $\mathrm{Jkg^{-1}\,K^{-1}}$), and T_v, the average virtual temperature of the consecutive measurements. Calculating pressure in iterative fashion

AMTD
6, 7771–7810, 2013

Propagation of radiosonde pressure sensor errors

R. M. Stauffer et al.

CC BY

from measurement-to-measurement throughout the profile reduces the error that use of a standard atmosphere or scale height would introduce. Since the uncertainty in the GPS altitude is small, usually within ±20 m (quoted in Vaisala RS92 technical specifications testing) to ±30 m (quoted in iMet radiosonde 2σ error specifications), the uncertainty of the calculated p_{GPS} will be quite small in the stratosphere. An additional source of uncertainty in p_{GPS} results from errors and biases in radiosonde temperature and humidity measurements, but is also considered quite small compared to the errors in radiosonde pressure measurements. This calculation assumes that the atmosphere is in hydrostatic balance with a pressure dependence only in the vertical. The radiosonde makes the same assumption when deriving a geopotential height from the pressure measurements through use of the hypsometric equation.

An example of the differences in radiosonde pressure (herein p) and p_{GPS} (treated as the reference), as well as the pressure altitude and GPS altitude differences are shown in Fig. 1. Large differences, on the order of several hundred meters, between pressure altitude and GPS altitude are an indication of systematic errors in reported pressures. For the remainder of this paper, we define the pressure offset to be $p - p_{\mathrm{GPS}}$.

Variability in the pressure offset appears in the lower troposphere since a difference of just a few meters between the GPS and the pressure altitude can cause several tenths of 1 hPa difference between the calculated and measured pressures. The noise in the pressure offset stabilizes in the stratosphere and often times monotonically increases until balloon burst.

2.4 Recalculating of pressure-dependent data

Using the pressure calculated from the GPS measurements, any pressure-dependent variables can be recalculated and compared to the original measurements. In addition to the reported altitude and pressure differences between the GPS and radiosonde measurements, we examine the effects on the O_{3MR} and total column O_3. (Note that the pressure corrections implemented here also result in a need to recalculate potential

AMTD
6, 7771–7810, 2013

Propagation of radiosonde pressure sensor errors

R. M. Stauffer et al.

temperature and, to a lesser extent, water vapor mixing ratio, but we do not discuss those here.)

The recalculation of O_{3MR} causes differences in both the O_3 magnitude and profile shape, particularly near the burst altitude and above 26 km (Fig. 2). Depending on the severity of the pressure offset, O_{3MR} errors can approach ±1–2 ppmv (parts per million by volume; ±10–20 % error) or greater in the stratosphere, a region critical for O_3 trend analyses and validation of satellite O_3 retrievals. Differences between GPS altitude and pressure altitude can cause the apparent O_{3MR} maximum to shift by as much as ±2 km, having further consequences for stratospheric satellite measurements and comparison/validation studies with ozonesondes.

We note that a pressure-dependent pump correction factor (PCF) is applied to pO_3 based on decreasing ozonesonde pump efficiency in the stratosphere, particularly above 25 km (Johnson et al., 2002). However, both the application of various PCFs in different processing software and the miniscule (~ 0.5 % difference in PCF between 20 and 18 hPa, near where statistics from this paper are presented) difference the PCF has between p and p_{GPS} profiles lead us to neglect this small correction.

3 Results

The IONS-06 campaign in August–September of 2006 provided an opportunity to compare coincident O_3 profiles from the University of Houston Main Campus (UH) and RHB, operated by NOAA to record profiles near the Houston Ship Channel and in Galveston Bay. The comparisons allow us to test confidence in the p_{GPS} recalculation procedure, namely the reproducibility of stratospheric O_{3MR} using ozonesondes with different radiosonde types released closely in space and time. Nine such pairs occurred within 90 min of each other in IONS-06, with RHB launching RS92s and the UH site launching RS80s with a separate GPS unit on board. An example of one pair, 15 min and 77 km apart on 30 August 2006 is shown in Fig. 3. The two profiles show similar tropospheric O_{3MR} with or without correcting the pressure offset (the p and p_{GPS}

AMTD
6, 7771–7810, 2013

Propagation of radiosonde pressure sensor errors

R. M. Stauffer et al.

profiles are indistinguishable below ∼15 km). The GPS corrected pressure, however, results in better agreement in stratospheric O_{3MR}. Mixing ratio differences between the two flights are greater than 1 ppmv near the UH balloon burst altitude (also note the altitude shift; Fig. 3), but are markedly closer and within 0.1–0.2 ppmv after correction of both profiles using p_{GPS}. Both the shift in the altitude and correction of the O_{3MR} contribute to this improved agreement.

3.1 Statistical characteristics of the pressure offsets

The median pressure offset for each km altitude bin (as in Hurst et al., 2011) from 1–30 km is shown in Fig. 4. The tight grouping of RS92 launches about the zero line is very noticeable, with considerably more spread near the top of the profiles measured with the other radiosonde types. All radiosondes show less variable pressure offsets in the stratosphere, with the RS92s converging to zero. The iMet-P radiosondes exhibit a peculiar S-shape pressure offset peak around 5 km that is not understood (no artifact or geophysical cause of which we are aware).

At 26 km (an altitude 82 % of profiles reach, also chosen because $p \approx 20$ hPa at 26 km), the iMet and RS80 radiosondes exhibit the most variable pressure offsets, with mean offsets of −0.65 hPa (−1.42 hPa 10th percentile; +0.69 hPa 90th percentile) and −0.55 hPa (−2.02 hPa; +0.51 hPa), respectively (Table 3). In Fig. 5, we see the radiosonde-measured pressure is consistently lower than p_{GPS} for many of the radiosonde types. The least variability is exhibited by the RS92s with only a +0.32 hPa (−0.09 hPa; +0.54 hPa) offset and just one outlier profile beyond ±1.0 hPa above 26 km.

Figure 6 shows pressure offsets at various altitudes as a function of the pressure offset at the burst altitude. The variance within the figure at different altitudes implies that the pressure offsets are not constant throughout most of the profile, and that a constant pressure correction cannot be applied to the entire profile. Only when the balloon reaches the stratosphere and around 15–20 km is a strong relationship evident. The tropospheric offsets appear much less constant than the stratospheric offsets, likely

CC BY

from variability in the GPS height and pressure sensor causing significant noise in the pressure offset below 10 km. As a result, the true magnitude of the pressure offset cannot be determined until well into the balloon flight, when GPS altitude and pressure altitude can be compared (see Appendix A, Fig. A1 for altitude differences with pressure offset) to assess potential pressure differences and the need for reprocessing.

3.2 O_{3MR} offsets

Pressure offsets of only a few tenths of 1 hPa are the equivalent of 5–10 % errors in the total atmospheric pressure near the balloon burst altitude. This pressure offset error results in an error in the calculated O_{3MR} of the same magnitude (Fig. 7). We define the O_{3MR} offsets as $[O_{3MR(p)} - O_{3MR(GPS)}]/O_{3MR(GPS)}$. Figure 7 demonstrates how a nearly constant stratospheric pressure offset results in an O_{3MR} offset that grows in magnitude with altitude, with many profiles beyond ±10 % error in the stratosphere. At such magnitudes, this error becomes a substantial component of the overall error budget associated with O_3 profile data from ozonesondes, and is beyond the intrinsic uncertainty of the O_3 measurements.

Table 3 examines the O_{3MR} errors by manufacturer. As with the pressure offsets, the most variable O_{3MR} percent offsets are displayed by the iMet and RS80 radiosondes with +3.81 % (–2.92 %; +7.00 %) and +2.75 % (–2.15 %; +9.19 %), at 26 km respectively. The iMet-P launches have an average offset at 26 km of +6.71 % that increases to +12.8 % by 30 km, leading to an average error nearing 1 ppmv O_{3MR} by balloon burst in a region critical for determining stratospheric O_3 trends.

Two distinct offset regimes are detected in the RS92s in Figs. 5 and 7, separable mainly by the launch sites Beltsville (one summer of data) and RHB near Galveston Bay (single campaign, see Appendix A, Figs. A2 and A3 for pressure and O_{3MR} offsets by launch site) with the Beltsville launches lying slightly to the left of the zero line, and RHB to the right. Similar offset groupings are also observed in the campaign-based launches from Porterville, CA (iMet, only one iMet-S), Las Tablas, Panama (RS80) and the set of iMet-P sondes launched in the course of 10 months at Idabel and Houston.

AMTD
6, 7771–7810, 2013

CC BY

This suggests that particular "batches" of radiosondes, regardless of manufacturer, may have offsets that generally behave in similar manners. The shelf life of the radiosondes are an additional factor to consider. Because of this, we caution against drawing conclusions about radiosonde types (particularly iMet-P radiosondes in this study) from offsets appearing in only one set or batch of sondes.

3.3 Column ozone measurements

Because the pressure offset affects both the apparent altitude and magnitude of O_{3MR}, it is also of interest to compute the influence on total column amount of O_3. Each of the 394 ozonesondes was integrated to obtain a column O_3 amount in Dobson Units (1 DU $= 2.69 \times 10^{16}$ molecules cm^{-2}) from both the original pressure profile and the recalculated p_{GPS} profile. As expected, considerable differences in the column integrated to the sonde burst altitude appear closely related to the pressure offset magnitude in the stratosphere (Fig. 8a) – the radiosonde types that displayed the largest pressure and O_{3MR} offsets also present the largest sonde column offsets. The iMet, iMet-P and RS80 sonde-only column O_3 differences are consistently ~ 10 DU too high prior to calculation of p_{GPS} (Table 3).

Adding a typical O_3 climatology (e.g., McPeters and Labow, 2012) above balloon burst allows calculation of total O_3 column abundance for both the original and pressure-corrected ozonesonde profiles. In this case, offsets are reduced to within a few DU (Fig. 9a). Note that sonde and/or satellite-based climatologies have become standard, replacing a constant mixing ratio assumption (McPeters et al., 1997, 2011; Thompson et al., 2003; McPeters and Labow, 2012; Morris et al., 2013). The sonde-only O_3 column discrepancies brought about by the differences in the balloon burst altitudes between the original and corrected pressure profiles is reconciled with the add-on above balloon burst and comparison of the total column O_3. The amount of total column offset is reduced to a mean offset within 4.1 DU for every radiosonde type with the above-burst addition (Table 3), signifying that both the O_{3MR} error and altitude differences are contributing to total column discrepancies.

AMTD
6, 7771–7810, 2013

A common practice within the ozonesonde community is to cut off total column O_3 integration at 10 hPa (Thompson et al., 2003, 2007), rather than integrating the entire profile, and to apply a climatology such as that of McPeters and Labow (2012) to the remainder. This is done for a variety of reasons including mitigation of increasing pump efficiency uncertainties with altitude in the stratosphere (Johnson et al., 2002) and the reduced accuracy of the O_3 measurements above 10 hPa (Komhyr et al., 1995b). The same technique was applied to the ozonesondes in this study to test if the sonde-only and total column O_3 offset is reduced due to elimination of increasing O_{3MR} errors routinely observed above 10 hPa.

The 10 hPa cut-off considerably reduces the differences between the uncorrected and pressure offset corrected sonde-only columns for every radiosonde type, except the iMet-P launches which in our data set rarely reached 10 hPa due to use of a smaller balloon (portions of the Houston and Idabel launches). For these launches, therefore, the entire balloon profile was integrated to the burst altitude. With the exception of the iMet-P sondes, sonde-only column O_3 average differences are reduced from a maximum of 9.3 DU to within 2.5 DU (Table 3, Fig. 8b). Considering the total column O_3 with the 10 hPa cut off and subsequent McPeters and Labow (2012) climatological add-on, the agreement between the uncorrected and corrected pressure O_3 columns is further improved and most differences are essentially noise within the uncertainty of the total column integration from the ozonesonde. All radiosonde types agree to an average offset within ±1 DU, with the poorest agreement from the iMet radiosonde 90th percentile of +3.3 DU (Table 3, Fig. 9b).

Figure 10 shows analysis of an individual profile to understand better the improved agreement in total column O_3 after the pressure correction is implemented. Figure 10 shows that the standard 10 hPa cut-off may provide a serendipitous solution to reconciling the differences between p and p_{GPS} total and sonde-only column O_3. The compensating effects of the pressure offset are viewed in terms of O_{3MR}, pO_3, and integrated sonde-only column with p and p_{GPS}. Because 10 hPa is above the pO_3 maximum in the stratosphere, the discrepancies on either side of the O_3 peak routinely compensate for

AMTD
6, 7771–7810, 2013

Propagation of radiosonde pressure sensor errors

R. M. Stauffer et al.

CC BY

one another when sonde integration is truncated (i.e., the column differences below the O_3 peak are negative (positive) while above the peak they are positive (negative)). Integrating to the burst altitude for those sondes that reach above 10 hPa results in poorer agreement with altitude – the further above 10 hPa the sonde reaches before burst, the greater the column error becomes. Thus it appears that the 10 hPa recommended limit for using the O_3 profile data results in a fortuitous minimization of the column errors caused by the pressure offsets and therefore our analysis argues in favor of the application an O_3 climatology such as that used by McPeters and Labow (2012) above balloon burst, with a cut-off at 10 hPa if necessary.

4 Summary and recommendations

A total of 501 radiosondes were compared to quantify errors in radiosonde pressure sensor measurements relative to pressure calculated from GPS measurements and to assess the impact these pressure offsets have on O_{3MR} and column O_3 measurements. The pressure offset was shown to detrimentally affect O_3 measurements, particularly in the stratosphere, where errors in O_{3MR} frequently exceed the laboratory uncertainty of the ozonesonde measurements of ±5 % in the lower stratosphere (Komhyr et al., 1995b). The performance of Vaisala RS92 radiosondes was superior to RS80s and three series of iMet radiosondes, and was characterized by offsets of only ±0.1–0.2 hPa at balloon burst, translating to O_{3MR} errors generally within ±1–2 % at 26 km.

The differences between the radiosonde-measured and GPS-calculated pressures also introduced an altitude shift in the profile that must be considered for satellite validation studies and column O_3 integration. The ozonesonde-only column exhibited a robust relationship with 26 km pressure offsets; sonde column differences between p and p_{GPS}-corrected profiles often exceeded +10 DU, or ∼ 3 % of the total column when offsets were beyond +1.0 hPa at 26 km. These column differences were reduced with the application of the above-balloon burst altitude O_3 climatology of McPeters and Labow (2012). When an integration cut-off of 10 hPa was applied the agreement improved to

AMTD
6, 7771–7810, 2013

CC BY

within a few DU. The improved agreement between the uncorrected and corrected total O_3 columns using a standard profile climatology and the 10 hPa cut-off argues for adopting this technique for column abundance estimates, especially with ozonesondes launched without GPS technology. Note that in the absence of GPS verification of the pressure profiles and O_{3MR}, this cut-off technique only improves the resulting calculated column abundance and does not improve the accuracy of the O_3 profile shape or O_{3MR} profile magnitude.

The ozonesonde community is currently in the process of homogenizing data (Deshler, 2012), seeking the highest accuracy trends and measurements, particularly at altitudes where satellite validation plays a vital role, from a global dataset spanning dozens of stations and up to 40 yr of measurements. The homogenization process will take into account sources of discrepancies and biases between different ozonesonde manufacturers, potassium iodide sensing solution strengths, and pump efficiency corrections. The pressure offset introduces an additional source of error (often significant) that is independent of the ozonesonde partial pressure measurement, and an error that is not constant, either with altitude or within a specific radiosonde type/manufacturer. It is anticipated that the analyses here will contribute to pressure corrections required as part of the ozonesonde data reprocessing.

The results of this study suggest the following recommendations regarding the pressure offset:

1. Ozonesondes should always be launched with a GPS-enabled radiosonde to ensure an accurate O_{3MR} magnitude and profile shape.

2. Pressure-dependent variables should be recalculated using p_{GPS}, especially when pressure offsets exceed ±1.0 hPa or ±5 % of the total atmospheric pressure at 26 km/20 hPa.

3. An above-burst climatology such as that used by McPeters and Labow (2012) should be applied using a 10 hPa cut-off (if applicable), particularly with ozonesondes launched prior to the GPS era for column abundance observation.

4. The statistics of this study can be used to guide recalculation of pressure and O_3 profiles taken prior to the adoption of GPS technology.

Appendix A

Extremely noisy pressure data from the Porterville, CA iMet radiosondes required smoothing prior to calculation and comparison of p_{GPS} and O_{3MR} (Fig. A1). This pressure noise introduced another source of error unrelated to the pressure offset for those 25 profiles (Table 1). The pressure data were first log transformed, then linearly interpolated every five seconds to obtain a smooth pressure profile. The data were then reverted to the exponential pressure profile and pressure-dependent variables were recalculated.

The effect the pressure offset has on the difference between radiosonde-reported geopotential height and GPS height is presented in Fig. A2. Using standard gravity, g_o, it is seen how a pressure offset of ±1.0 hPa (frequently observed in this study) can lead to an altitude discrepancy of ±1.0–1.5 km, having major implications for column O_3 and the shifting of O_3 profile shape.

The pressure offset ($p - p_{GPS}$) and O_{3MR} offset ($[O_{3MR(p)} - O_{3MR(GPS)}]/O_{3MR(GPS)}$) by launch site are shown in Figs. A3 and A4. As mentioned in Sect. 3.2, similar offset groupings are observed in the campaign-based launches from Porterville, CA, Las Tablas, Panama and at Idabel and Houston which launched iMet-P sondes in the course of 10 months in 2012/2013.

Acknowledgements. This work was supported by grants NNX09AJ236 (SHADOZ), NNX10AR39G (DISCOVER-AQ), and NNX12AF056 to Penn State University with additional support to Anne Thompson from the US – South Africa Fulbright Scholar Program (2010–2011). Funding for Gary Morris was provided by a Fulbright Scholar Grant from the Japan – US Educational Commission, NASA's Division of Earth Science Aura Data Validation Program (D. Considine and E. Hilsenrath, program managers), INTEX-B Mission, and TC^4 Mission, and the Texas Commission for Environmental Quality. Special thanks to hosts in Japan during Gary

Morris' Fulbright: June Hirokawa and Fumio Hasebe (Hokkaido University, Sapporo, Japan) and Hajime Akimoto (Frontier Research Center for Global Change, Yokohama, Japan). Thanks also to Barry Lefer at University of Houston (Houston, TX) and Bob Heinemann at the Oklahoma State University Kiamichi Forestry Research Station (Idabel, OK) and to the many students who have been involved in the ozonesonde launches from the various sites over the years. Access to Beltsville data was facilitated by Cassie Stearns at the Howard University Beltsville Center for Climate Studies and Observation. Thanks to Frederick Clowney at International Met Systems for additional information and assistance.

References

da Silveira, R. B., Fisch, G. F., Machado, L. A. T., Dall'Antonia, A. M., Sapucci, L. F., Fernandes, D., Marques, R., and Nash, J.: WMO Intercomparison of GPS Radiosondes, WMO/TD-No. 1314, available at: http://www.wmo.int/pages/prog/www/IMOP/publications/IOM-90_RSO-Brazil/IOM-90_RSO_EMA_Alcantara2001.pdf, Alcantara, Brazil, 20 May–10 June 2001, 65 pp., 2006.

Deshler, T., Mercer, J. L., Smit, H. G. J., Stubi, R., Levrt, G., Johnson, B. J., Oltmans, S. J., Kivi, R., Thompson, A. M., Witte, J. C., Davies, J., Schmidlin, F. J., Brothers, G., and Sasaki, T.: Atmospheric comparison of electrochemical cell ozonesondes from different manufacturers, and with different cathode solution strengths: the balloon experiment on standards for ozonesondes, J. Geophys. Res., 113, D04307, doi:10.1029/2007JD008975, 2008.

Deshler, T.: Transfer functions for SPC6A-ENSCI-SST1% and SST0.5%, available at: http://www-das.uwyo.edu/~deshler/NDACC_O3Sondes/O3s_DQA/O3S-DQA-8.1.2_sst1_vs_sst0.5&spc_vs_ensci.pdf (last access: 25 July, 2013), 2012.

Dobson, G. M. B.: Atmospheric ozone and the movement of air in the stratosphere, Pure Appl. Geophys., 106–108, 1520–1530, doi:10.1007/BF00881102, 1973.

Froidevaux, L., Read, W. G., Lungu, T. A., Cofield, R. E., Fishbein, E. F., Flower, D. A., Jarnot, R. F., Ridenoure, B. P., Shippony, Z., Waters, J. W., Margitan, J. J., McDermid, I. S., Stachnik, R. A., Peckham, G. E., Braathen, G., Deshler, T., Fishman, J., Hofmann, D. J., and Oltmans, S. J.: Validation of UARS microwave limb sounder ozone measurements, J. Geophys. Res., 101, 10017–10060, doi:10.1029/95JD02325, 1996.

AMTD

6, 7771–7810, 2013

Propagation of radiosonde pressure sensor errors

R. M. Stauffer et al.

CC BY

Gaffen, D. J.: Temporal inhomogeneities in radiosonde temperature records, J. Geophys. Res., 99, 3667–3676, doi:10.1029/93JD03179, 1994.

Gaffen, D. J., Sargent, M. A., Habermann, R. E., and Lanzante, J. R.: Sensitivity of tropospheric and stratospheric temperature trends to radiosonde data quality, J. Climate, 13, 1776–1796, doi:10.1175/1520-0442(2000)013<1776:SOTAST>2.0.CO;2, 2000.

Hurst, D. F., Hall, E. G., Jordan, A. F., Miloshevich, L. M., Whiteman, D. N., Leblanc, T., Walsh, D., Vömel, H., and Oltmans, S. J.: Comparisons of temperature, pressure and humidity measurements by balloon-borne radiosondes and frost point hygrometers during MOHAVE-2009, Atmos. Meas. Tech., 4, 2777–2793, doi:10.5194/amt-4-2777-2011, 2011.

Inai, Y., Hasebe, F., Shimizu, K., and Fujiwara, M.: Correction of radiosonde pressure and temperature measurements using simultaneous GPS height data, SOLA, 5, 109–112, doi:10.2151/sola.2009-028, 2009.

IPCC – International Panel on Climate Change: Climate Change 2007: the Physical Science Basis, Contribution of Working Group I to the Fourth Assessment Report of the Intergovernmental Panel on Climate Change, edited by: Solomon, S., Qin, D., Manning, M., Chen, Z., Marquis, M., Averyt, K. B., Tignor, M., and Miller, H. L., Cambridge University Press, Cambridge, UK and New York, NY, USA, 996 pp., 2007.

Jiang, Y. B., Froidevaux, L., Lambert, A., Livesey, N. J., Read, W. G., Waters, J. W., Bojkov, B., Leblanc, T., McDermid, I. S., Godin-Beekmann, S., Filipiak, M. J., Harwood, R. S., Fuller, R. A., Daffer, W. H., Drouin, B. J., Cofield, R. E., Cuddy, D. T., Jarnot, R. F., Knosp, B. W., Perun, V. S., Schwartz, M. J., Snyder, W. V., Stek, P. C., Thurstans, R. P., Wagner, P. A., Allaart, M., Andersen, S. B., Bodeker, G., Calpini, B., Claude, H., Coetzee, G., Davies, J., De Backer, H., Dier, H., Fujiwara, M., Johnson, B., Kelder, H., Leme, N. P., König-Langlo, G., Kyro, E., Laneve, G., Fook, L. S., Merrill, J., Morris, G., Newchurch, M., Oltmans, S., Parrondos, M. C., Posny, F., Schmidlin, F., Skrivankova, P., Stubi, R., Tarasick, D., Thompson, A., Thouret, V., Viatte, P., Vömel, H., von Der Gathen, P., Yela, M., and Zablocki, G.: Validation of aura microwave limb sounder ozone by ozonesonde and lidar measurements, J. Geophys. Res., 112, D24S34, doi:10.1029/2007JD008776, 2007.

Johnson, B. J., Oltmans, S. J., Vömel, H., Smit, G. J., Deshler, T., and Kröger, C.: Electrochemical concentration cell (ECC) ozonesonde pump efficiency measurements and tests on the sensitivity to ozone of buffered and unbuffered ECC sensor cathode solutions, J. Geophys. Res., 107, 4393, doi:10.1029/2001JD000557, 2002.

Komhyr, W. D.: Electrochemical concentration cells for gas analysis, Ann. Geophys., 25, 203–210, 1969, http://www.ann-geophys.net/25/203/1969/.
Komhyr, W. D., Connor, B. J., McDermid, I. S., McGee, T. J., Parrish, A. D., and Margitan, J. J.: Comparison of STOIC ground-based lidar, microwavespectrometer, and Dobson spectrophotometer Umkehr ozone profiles with ozone profiles from balloon-borne electrochemical concentration cell ozonesondes, J. Geophys. Res., 100, 9273–9282, doi:10.1029/94JD02173,1995a.
Komhyr, W. D., Barnes, R. A., Brothers, G. B., Lathrop, J. A., and Opperman, D. P.: Electrochemical concentration cell ozonesonde performance evaluation during STOIC 1989, J. Geophys. Res., 100, 9231–9244, doi:10.1029/94JD02175, 1995b.
Kroon, M., de Haan, J. F., Veefkind, J. P., Froidevaux, L., Wang, R., Kivi, R., and Hakkarainen, J. J.: Validation of operation ozone profiles from the Ozone Monitoring Instrument, J. Geophys. Res., 116, D18305, doi:10.1029/2010JD015100, 2011.
Liu, X., Chance, K., Sioris, C. E., Kurosu, T. P., and Newchurch, M. J.: Intercomparison of GOME, ozonesonde, and SAGE II measurementsof ozone: demonstration of the need to homogenize available ozonesonde data sets, J. Geophys. Res., 111, D14305, doi:10.1029/2005JD006718, 2006.
Logan, J. A.: Trends in the vertical distribution of ozone: an analysis of ozonesonde data, J. Geophys. Res., 99, 25553–25585, doi:10.1029/94JD02333, 1994.
Logan, J. A., Megretskaia, I. A., Miller, A. J., Tiao, G. C., Choi, D., Zhang, L., Stolarski, R. S., Labow, G. J., Hollandsworth, S. M., Bodeker, G. E., Claude, H. De Muer, D., Kerr, J. B., Tarasick, D. W., Oltmans, S. J., Johnson, B. J., Schmidlin, F., Staehelin, J., Viatte, P., and Uchino, O.: Trends in the vertical distribution of ozone: a comparison of two analyses of ozonesonde data, J. Geophys. Res., 104, 26373–26399, doi:10.1029/1999JD900300, 1999.
McPeters, R. D. and Labow, G. J.: Climatology 2011: an MLS and sonde derived ozone climatology for satellite retrieval algorithms, J. Geophys. Res., 117, D10303, doi:10.1029/2011JD017006, 2012.
McPeters, R. D., Labow, G. J., and Johnson, B. J.: A satellite-derived ozone climatology for balloonsonde estimation of total column ozone, J. Geophys. Res., 102, 8875–8885, doi:10.1029/96JD02977, 1997.
McPeters, R. D., Labow, G. J., and Logan, J. A.: Ozone climatological profiles for satellite retrieval algorithms, J. Geophys. Res., 112, D05308, doi:10.1029/2005JD006823, 2007.

CC BY

Miller, A. J., Tiao, G. C., Reinsel, G. C., Wuebble, D., Bishop, L., Kerr, J., Nagatani, R. M., DeLuisi, J. J., and Mateer, C. L.: Comparisons of observed ozone trends in the stratosphere through examination of Umkehr and balloon ozonesonde data, J. Geophys. Res., 100, 11209–11217, doi:10.1029/95JD00632, 1995.

Miloshevich, L. M., Vömel, H., Whiteman D. N., Lesht, B. M., Schmidlin, F. J., and Russo, F.: Absolute accuracy of water vapor measurements from six operational radiosonde types launched during AWEX-G and implications for AIRS validation, J. Geophys. Res., 111, D09S10, doi:10.1029/2005JD006083, 2006.

Morris, G. A., Labow, G., Akimoto, H., Takigawa, M., Fujiwara, M., Hasebe, F., Hirokawa, J., and Koide, T.: On the use of the correction factor with Japanese ozonesonde data, Atmos. Chem. Phys., 13, 1243–1260, doi:10.5194/acp-13-1243-2013, 2013.

Nalli, N. R., Barnet, C. D., and Reale, T.: Validation of infrared sounder Environmental Data Records: application to the Cross-track Infrared Microwave Sounder Suite (CrIMSS), manuscript in review for Special Section on NPP Cal/Val Science Results, J. Geophys. Res.-Atmos., in review, 2013.

Nash, J., Smout, R., Oakley, T., Pathack, B., and Kurnosenko, S.: WMO intercomparison of high quality radiosonde systems, 2–25 February 2005, WMO/TD-No. 1303, available at: http://www.wmo.int/pages/prog/www/IMPO/publications/IOM-83_RSO-Mauritius/IOM-83_Radiosondes_Vacoas2005.pdf, Vacoas, Mauritius, 115 pp., 2006.

National Imagery and Mapping Agency Technical Report: Department of Defense World Geodetic System 1984, available at: http://earth-info.nga.mil/GandG/publications/tr8350.2/wgs84fin.pdf (last access: 3 May 2013), 2000.

Osterman, G. B., Kulawik, S. S., Worden, H. M., Richards, N. A. D., Fisher, B. M., Eldering, A., Shephard, M. W., Froidevaux, L., Labow, G., Luo, M., Herman, R. L., Bowman, K. W., and Thompson, A. M.: Validation of Tropospheric Emission Spectrometer (TES) measurements of the total, stratospheric, and tropospheric column abundance of ozone, J. Geophys. Res., 113, D15S16, doi:10.1029/2007JD008801, 2008.

Rault, D. F. and Taha, G.: Validation of ozone profiles retrieved from Stratospheric Aerosol and Gas Experiment II limb scatter measurements, J. Geophys. Res., 112, D13309, doi:10.1029/2006JD007679, 2007.

Smit, H. G. J. and Berg, M.: JOSIE-2009/2010 experiments with ECC-ozone Sonde Types using different sensing solutions: the need for empirical transfer functions to resolve inhomogenities

cc BY

in time series, available at: http://igaco-o3.fmi.fi/VDO/presentations_2011/ground-based/WS_2011_Smit.pdf (last access: 25 July 2013), 2011.

Smit, H. G. J. and Kley, D.: JOSIE: The 1996 WMO International intercomparison of Ozonesondes under quasi Flight Conditions in the Environmental Simulation Chamber at Jülich, WMO Global Atmosphere Watch Report Series, No. 130, Technical Document No. 926, World Meteorological Organization, Geneva, 1998.

Smit, H. G. J., Straeter, W., Johnson, B. J., Oltmans, S. J., Davies, J., Tarasick, D. W., Hoegger, B., Stubi, R., Schmidlin, F. J., Northam, T., Thompson, A. M., Witte, J. C., Boyd, I., and Posny, F.: Assessment of the performance of ECC-ozonesondes under quasi-flight conditions in the environmental simulation chamber: insights from the Juelich Ozone Sonde Intercomparison Experiment (JOSIE), J. Geophys. Res.-Atmos., 112, D19306, doi:10.1029/2006JD007308, 2007.

Steinbrecht, W., Claude, H., Schönenborn, F., Leiterer, U., Dier, H., and Lanzinger, E.: Pressure and temperature differences between Vaisala RS80 and RS92 radiosonde systems, J. Atmos. Ocean. Tech., 25, 909–927, doi:10.1175/2007JTECHA999.1, 2008.

Sun, B., Reale, A., Seidel, D. J., and Hunt, D. C.: Comparing radiosonde and cosmic atmospheric profile data to quantify differences among radiosonde types and the effects of imperfect collocation on comparison statistics, J. Geophys. Res., 115, D23104, doi:10.1029/2010JD014457, 2010.

Thompson, A. M., Witte, J. C., McPeters, R. D., Oltmans, S. J., Schmidlin, F. J., Logan, J. A., Fujiwara, M., Kirchhoff, V. W. J. H., Posny, F., Coetzee, G. J. R., Hoegger, B., Kawakami, S., Ogawa, T., Johnson, B. J., Vömel, H., and Labow, G.: Southern Hemisphere Additional Ozonesondes (SHADOZ) 1998–2000 tropical ozone climatology: 1. Comparison with TOMS and ground-based measurements, J. Geophys. Res., 108, 8238, doi:10.1029/2001JD000967, 2003.

Thompson, A. M., Witte, J. C., Smit, H. G. J., Oltmans, S. J., Johnson, B. J., Kirchhoff, V. W. J. H., and Schmidlin, F. J.: Southern Hemisphere Additional Ozonesondes (SHADOZ) 1998–2004 tropical ozone climatology: 3. Instrumentation, station-to-station variability, and evaluation with simulated flight profiles, J. Geophys. Res., 112, D03304, doi:10.1029/2005JD007042, 2007.

Vömel, H., Selkirk, H., Miloshevich, L., Valverde-Canossa, J., Valdés, J., Kyrö, E., Kivi, R., Stolz, W., Peng, G., and Diaz, J. A.: Radiation dry bias of the Vaisala RS92 humidity sensor, J. Atmos. Ocean. Tech., 24, 953–962, doi:10.1175/JTECH2019.1, 2007.

WMO – World Meteorological Organization: Scientific Assessment of Ozone Depletion: 2010, Global Ozone Research and Monitoring Project – Report No. 52, Geneva, Switzerland, 516 pp., 2011.

WMO – World Meteorological Organization: Quality Assurance and Quality Control for Ozonesonde Measurements in GAW, Global Atmospheric Watch – Report No. 201, available at: http://www.wmo.int/pages/prog/arep/gaw/documents/GAW_201.pdf, Geneva, Switzerland, 100 pp., 2013.

Yoneyama, K., Fujita, M., Sato, N., Fujiwara, M., Inai, Y., and Hasebe, F.: Correction for radiation dry bias found in RS92 radiosonde data during the MISMO field experiment, SOLA, 4, 013–016, doi:10.2151/sola.2008-004, 2008.

AMTD
6, 7771–7810, 2013

CC BY

Table 1. Balloon launch locations with latitude/longitude coordinates, number of launches, radiosonde types used and lengths of records used in this study.

Location	Lat/Lon	Launches	Radiosonde Types	Length of Record
Irene, South Africa	−25.91°/28.21°	28	RS92	10 Sep 2012–17 Apr 2013
Las Tablas, Panama	7.75°/−80.25°	21	RS80	13 Jul 2007–8 Aug 2007
Houston, Texas (two locations)	29.72°/−95.34° 30.03°/−94.08°	147	RS80, iMet, iMet-P, iMet-S	1 Mar 2006–26 Jan 2013
Ronald H. Brown Vessel Gulf of Mexico	24.8° to 29.7°/−94.7° to −83.5°	37, 107 radiosonde-only	RS92	27 Jul 2006–11 Sep 2006
Idabel, Oklahoma	33.89°/−94.75°	40	iMet, iMet-P, iMet-S	18 Aug 2010–4 Oct 2012
Porterville, California	36.03°/−119.05°	25	iMet, iMet-S	16 Jan 2013–6 Feb 2013
Beltsville, Maryland	39.05°/−76.88°	16	RS92	27 Jun 2007–7 Aug 2007
Edgewood, Maryland	39.41°/−76.30°	36	iMet-S	28 Jun 2011–30 Jul 2011
Valparaiso, Indiana	41.46°/−87.04°	20	RS80	19 Apr 2006–3 Nov 2007
Sapporo, Japan	43.07°/141.35°	24	RS80	6 Aug 2008–4 Sep 2009

AMTD
6, 7771–7810, 2013

CC BY

Table 2. Radiosonde types with number of launches, quoted pressure uncertainties/accuracies from the manufacturer, and dates of available launches. We note the various iMet series have had no appreciable changes to the pressure sensors, but are split in these analyses for convenience and ease of interpretation.

Radiosonde Type	Launches	Quoted Pressure Uncertainty/Accuracy	Length of Record
iMet	61	1070–400 hPa: 1.8 hPa/400–4 hPa: 0.5 hPa[1]	28 May 2009–6 Feb 2013
iMet-P	44	1070–400 hPa: 1.8 hPa/400–4 hPa: 0.5 hPa[1]	23 Mar 2012–26 Jan 2013
iMet-S	53	1070–400 hPa: 1.8 hPa/400–4 hPa: 0.5 hPa[1]	4 Sep 2010–16 Jan 2013
RS80	155	1080–3 hPa: 1. hPa[2]	1 Mar 2006–23 Apr 2011
RS92	188	1080-100 hPa: 0.5 hPa/100–3 hPa: 0.3 hPa[2]	27 Jul 2006–17 Apr 2013

[1] The iMet values given are 2σ accuracy limits.
[2] The RS80 and RS92 values given are 2σ limits on sounding reproducibility.

AMTD
6, 7771–7810, 2013

Propagation of radiosonde pressure sensor errors

R. M. Stauffer et al.

Table 3. Various pressure and O_3 statistics separated by radiosonde type. All columns are presented in 10th percentile, mean and 90th percentile values. Values are reported as original pressure profile data minus GPS-calculated pressure profile data.

Radiosonde Type	Pressure Offset (hPa, 26 km)	O_{3MR} Error (%, 26 km)	Sonde Column Difference (to burst, DU)	Sonde Column Difference (to 10 hPa, DU)	Total Column Difference (to burst+add-on, DU)	Total Column Difference (to 10 hPa+add-on, DU)
iMet	−1.42, −0.65, 0.69	−2.92, 3.81, 7.00	−1.7, 9.5, 17.5	−1.7, 2.4, 5.9	0.0, 4.1, 7.3	−0.8, 1.1, 3.3
iMet-P	−2.33, −1.49, −0.82	3.61, 6.71, 11.0	3.8, 10.3, 15.0	3.8, 10.1, 14.9	−2.6, −0.9, 1.4	−2.6, −l.0, 1.4
iMet-S	−0.92, −0.13, 0.91	−3.56, 0.63, 3.78	−4.7, 2.9, 8.3	−4.3, 0.8, 5.7	−1., 1., 2.1	−0.7, 0.6, 1.8
RS80	−2.02, −0.55, 0.51	−2.15, 2.75, 9.19	−1.8, 7.8, 22.9	−1.9, 2.5, 10.2	−0.5, 2.5, 6.9	−1.0, 0.0, 2.0
RS92	−0.09, 0.32, 0.54	−2.19, −1.31, 0.37	−1.6, 0.0, 1.1	−0.9, 0.0, 0.7	−0.3, 0.3, 0.8	−0.1, 0.2, 0.8

AMTD
6, 7771–7810, 2013

CC BY

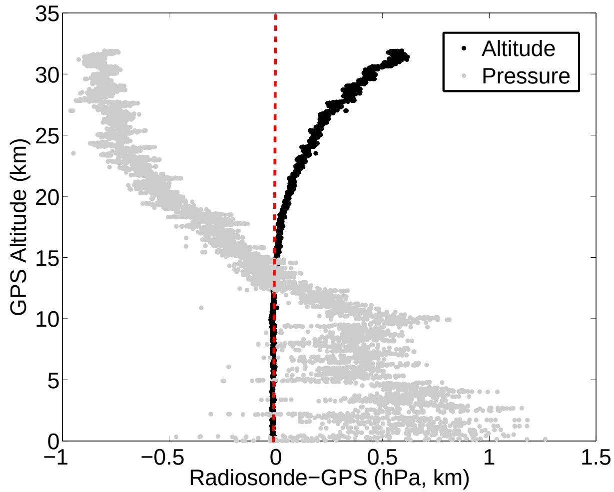

Fig. 1. Edgewood, MD iMet-S profile from 14 July 2011 of GPS and pressure altitude differences (black), and pressure differences after recalculation of pressure data from GPS measurements (grey). The red dashed line marks the zero line for reference.

AMTD
6, 7771–7810, 2013

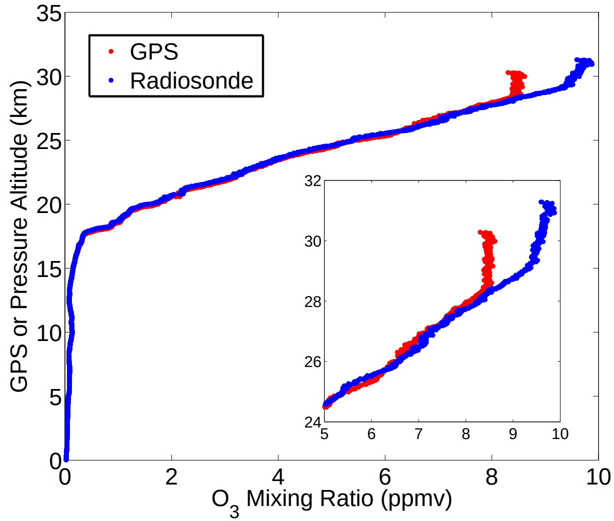

Fig. 2. Sapporo, Japan RS80 profile from 19 August 2008 showing original pressure (blue) and recalculated GPS pressure (red) O_{3MR} profiles. The inset figure is the same profile, zoomed-in to highlight O_3 differences in the stratosphere.

AMTD
6, 7771–7810, 2013

Propagation of radiosonde pressure sensor errors

R. M. Stauffer et al.

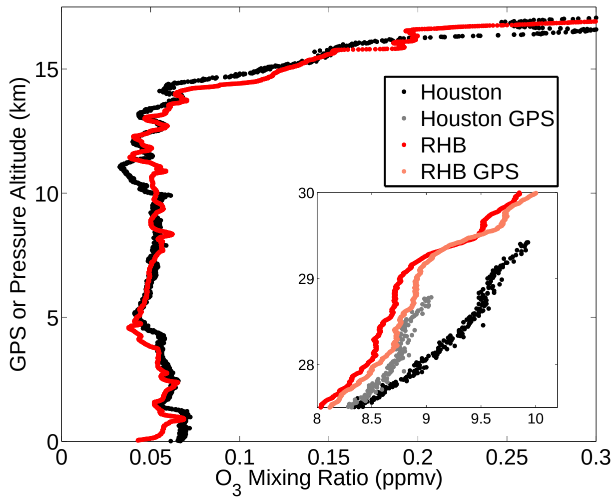

Fig. 3. Nearly coincident profiles from 30 August 2008 from the *Ronald H. Brown* (RS92), and Houston, TX (RS80). The original O_{3MR} profiles are shown in black (Houston) and red (RHB). The inset highlights improved stratospheric O_{3MR} agreement from the coincident RHB and TX profiles after GPS reprocessing with the corrected profiles from p_{GPS} shown in grey (Houston) and light red (RHB).

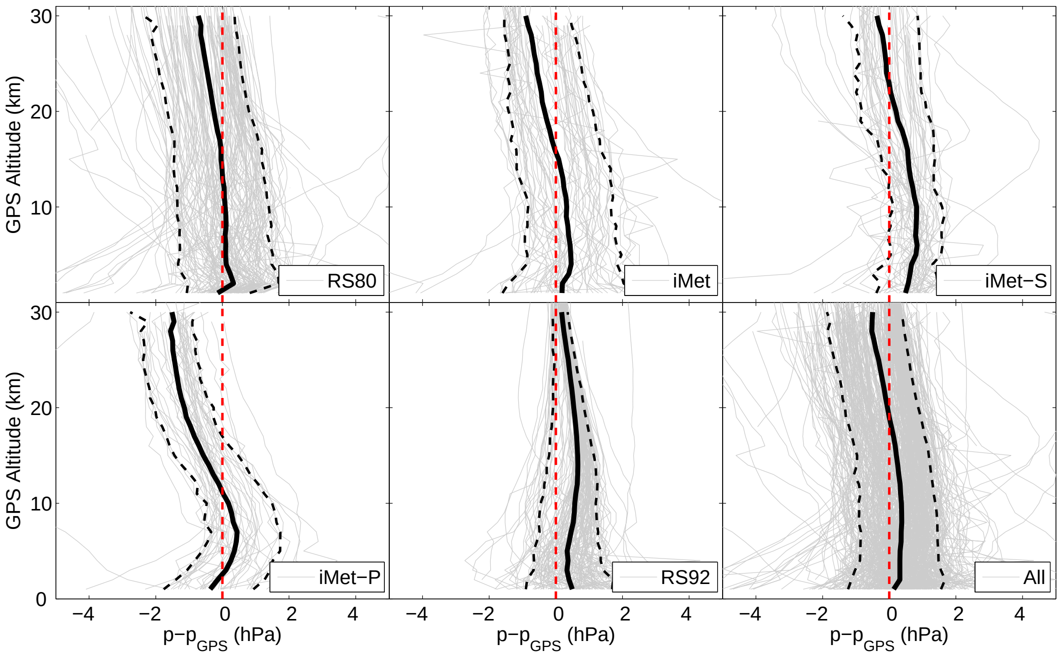

Fig. 4. Median pressure offset ($p - p_{GPS}$) for every 1 km altitude bin from 1–30 km for each radiosonde type (grey). Average offsets (black solid line) for each grouping of radiosondes are shown along with 10th and 90th percentiles (black dashes). A red dashed line marks the zero line for reference.

AMTD
6, 7771–7810, 2013

Propagation of radiosonde pressure sensor errors

R. M. Stauffer et al.

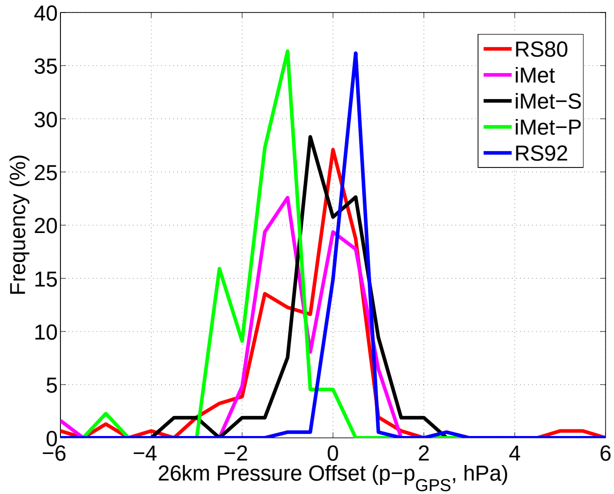

Fig. 5. Histogram of 26 km pressure offset in percent frequency by radiosonde type. Data are binned every 0.5 hPa.

CC BY

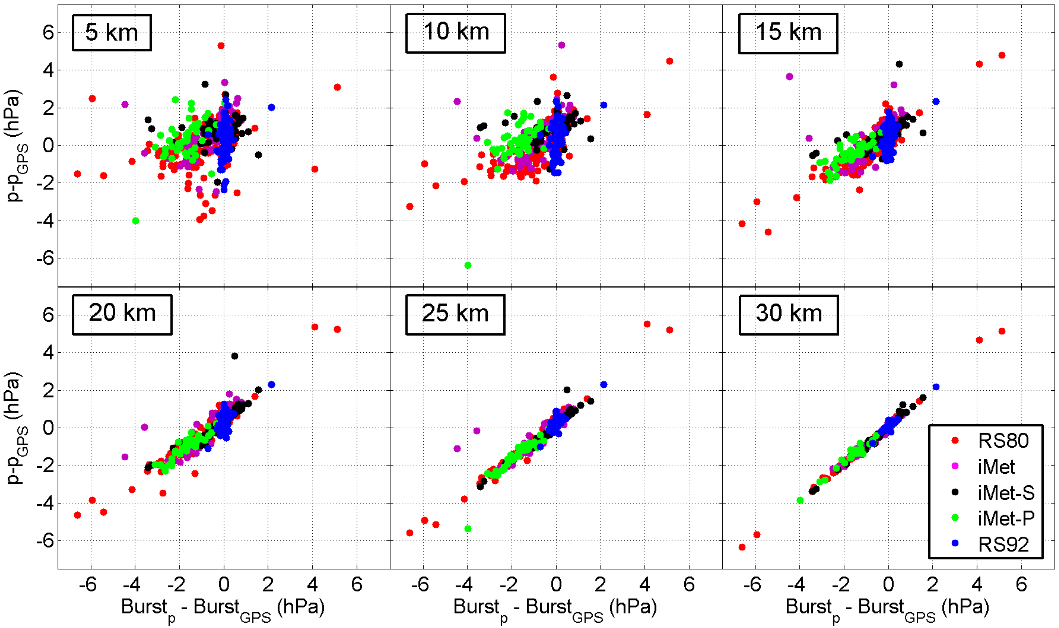

Fig. 6. Pressure offset at various altitudes vs. eventual pressure offset at burst by radiosonde type.

AMTD
6, 7771–7810, 2013

Propagation of radiosonde pressure sensor errors

R. M. Stauffer et al.

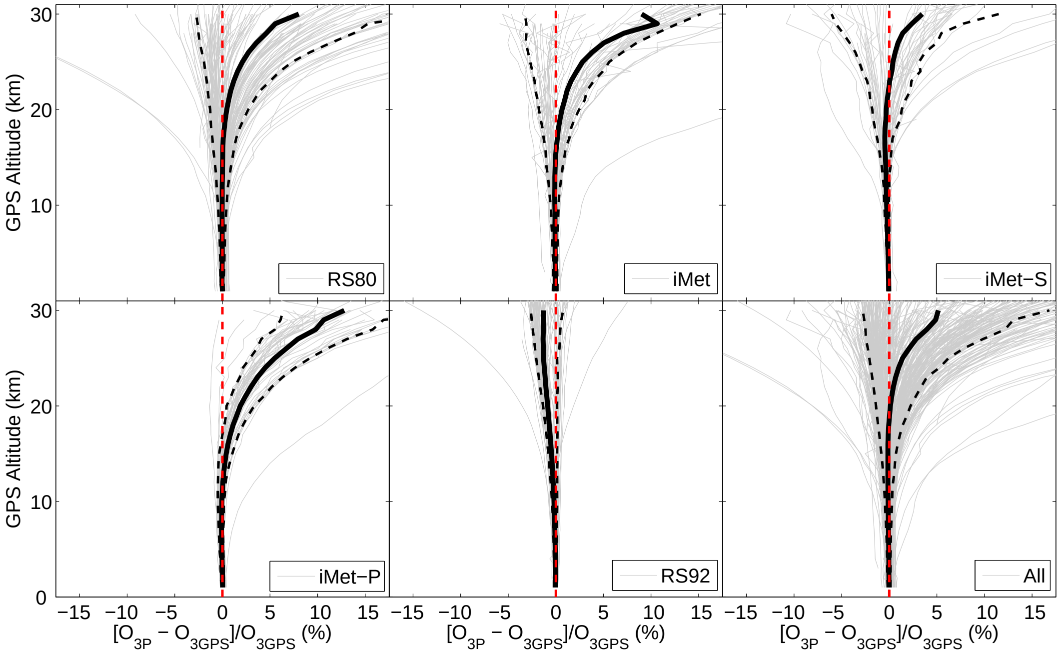

Fig. 7. Median percent O_{3MR} offset ($[O_{3p} - O_{3GPS}]/O_{3GPS}$) for every 1 km altitude bin from 1–30 km for each radiosonde type (grey). Average offsets (black solid line) for each grouping of radiosondes are shown along with 10th and 90th percentiles (black dashes). A red dashed line marks the zero line for reference.

AMTD
6, 7771–7810, 2013

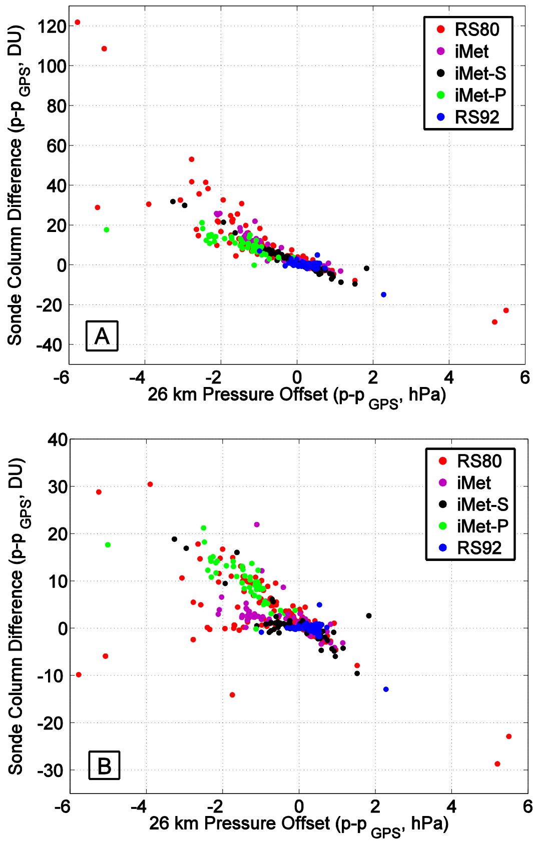

Fig. 8. Ozonesonde-only column O_3 using the difference of columns calculated with p and p_{GPS}, and with integration to burst **(A)** and cut off at 10 hPa **(B)** compared to the 26 km pressure offset ($p - p_{GPS}$). The various radiosonde types are identified by their respective colors. A few outliers were left from the figure for clarity.

AMTD
6, 7771–7810, 2013

Propagation of radiosonde pressure sensor errors

R. M. Stauffer et al.

Title Page
Abstract Introduction
Conclusions References
Tables Figures
◀ ▶
Back Close
Full Screen / Esc
Printer-friendly Version
Interactive Discussion

CC BY

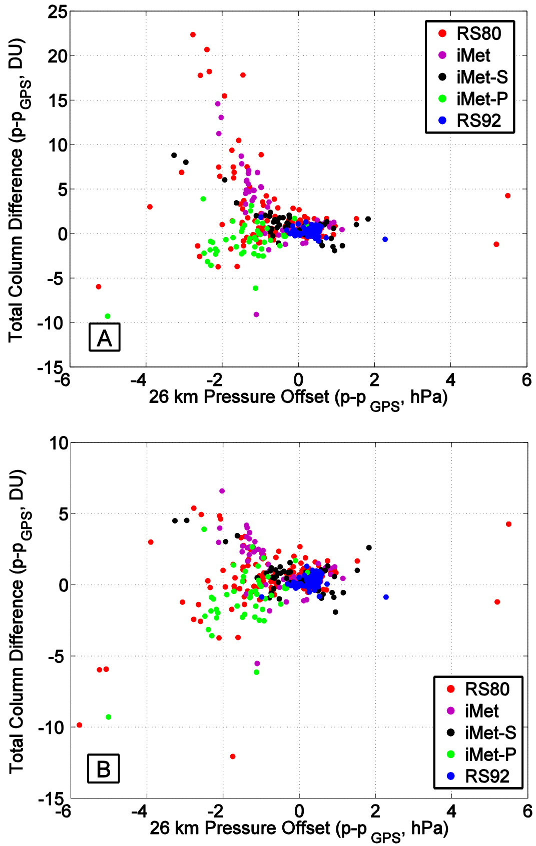

Fig. 9. As Fig. 8 except the McPeters and Labow (2012) above-burst O_3 climatology was added to each sonde from **(A)** burst or **(B)** 10 hPa/burst if greater than 10 hPa.

AMTD
6, 7771–7810, 2013

Propagation of radiosonde pressure sensor errors

R. M. Stauffer et al.

CC BY

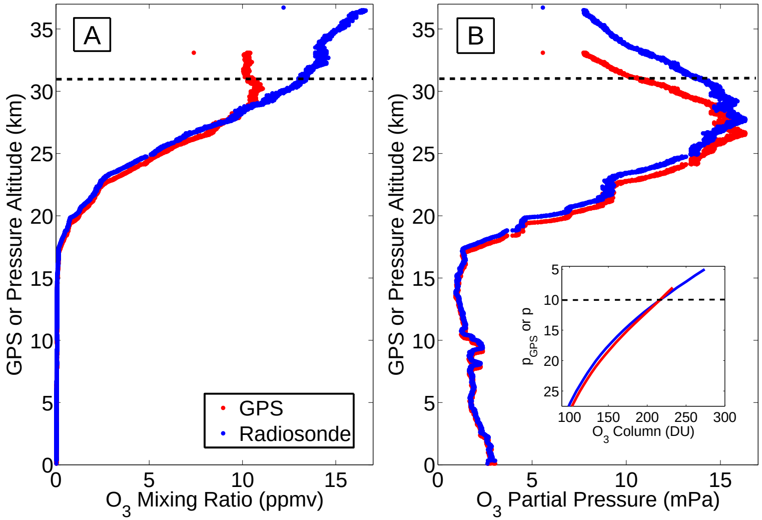

Fig. 10. Las Tablas, Panama RS80 sounding from 31 July 2007 showing GPS (red) and radiosonde (blue) profiles of O_{3MR} **(A)** and pO_3 **(B)**. The inset in **(B)** is integrated ozonesonde column showing compensating differences causing agreement in column O_3 by 10 hPa. The 10 hPa cut-off used prior to adding the McPeters and Labow (2012) O_3 climatology is marked by the black dashed line on all plots.

AMTD
6, 7771–7810, 2013

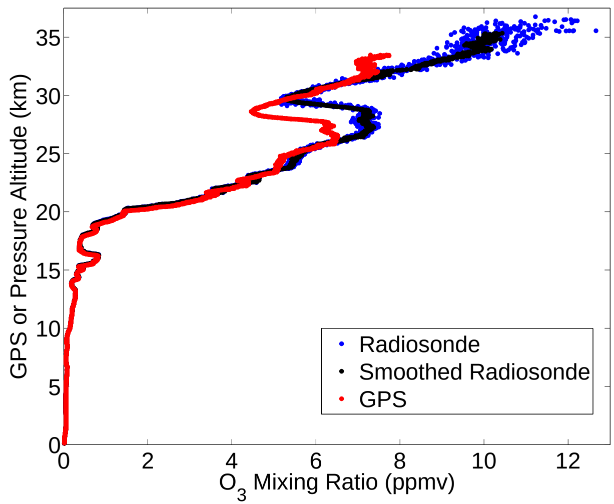

Fig. A1. Porterville, CA iMet profile from 24 January 2013 showing the results of first smoothing the original (blue) O_{3MR} data, then recalculating the smoothed O_{3MR} (black) with p_{GPS} to obtain the corrected O_3 profile (red).

AMTD
6, 7771–7810, 2013

CC BY

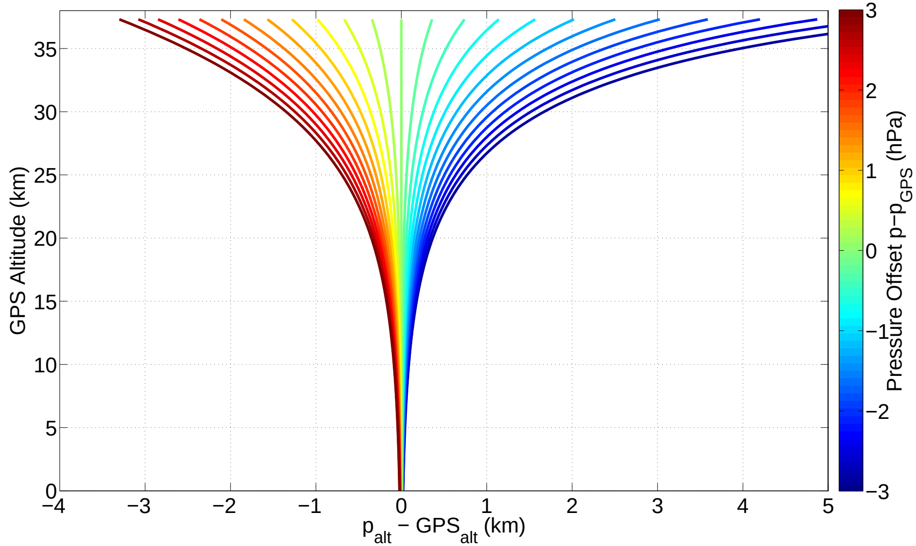

Fig. A2. Altitude differences between pressure and GPS altitude with GPS height based on magnitude of pressure offset. Pressure offsets from −3 to 3 hPa in increments of 0.25 hPa were plotted. This calculation assumes a scale height of ~7000 m ($\overline{T}_v = 240$ K, $g = g_0 = 9.80665$ ms^{-2}), and was calculated from $p_{GPS} = 1013$ to 5 hPa.

AMTD
6, 7771–7810, 2013

CC BY

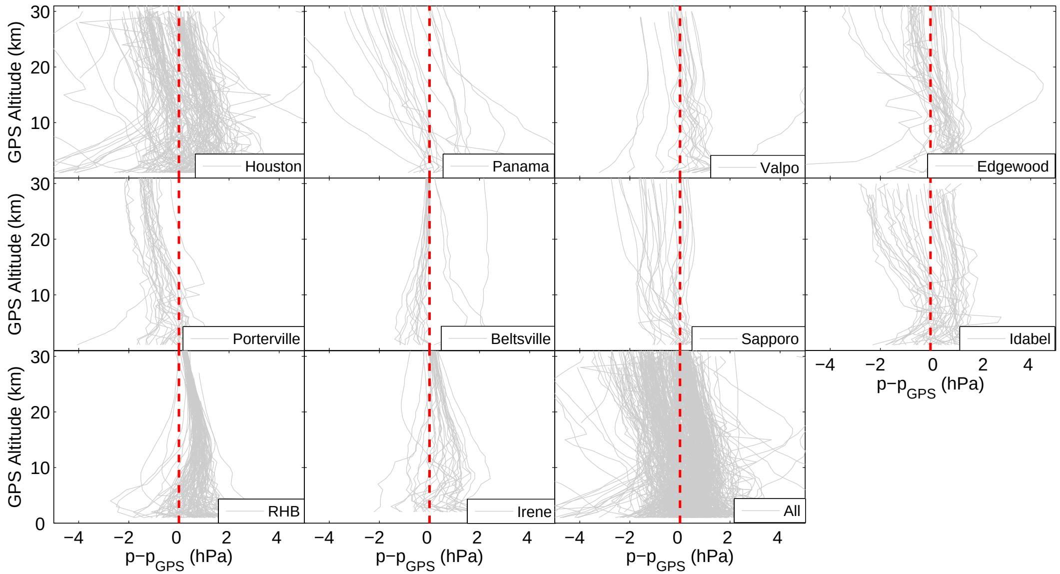

Fig. A3. Pressure offset ($p - p_{GPS}$) by launch site. A red dashed line marks the zero line for reference.

AMTD

6, 7771–7810, 2013

Propagation of radiosonde pressure sensor errors

R. M. Stauffer et al.

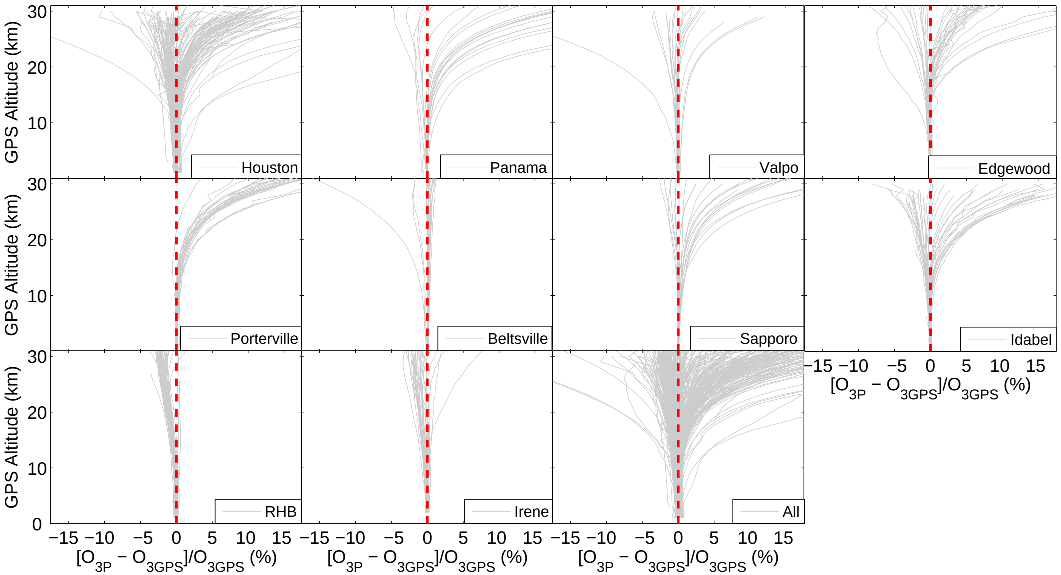

Fig. A4. Percent O_{3MR} offset ($[O_{3p} - O_{3GPS}]/O_{3GPS}$) by launch site. A red dashed line marks the zero line for reference.

AMTD
6, 7771–7810, 2013